# RESEARCH ON DEM CALIBRATION OF CONTACT PARAMETERS OF SWEET SORGHUM SEED
/
# 甜高粱种子离散元接触参数标定研究

**Jin YANG[1)], Zhen WANG[1)], Xin DU*[1,2)], Qixin SUN[1)]**
[1)]School of Mechanical Engineering, Jiangsu Ocean University, Lianyungang 222005 / China;
[2)] Lianyungang Zhiyun Mechanical Equipment Technology Co., Ltd., Lianyungang 222001 / China;
*Tel: 0086-0518-85895322; E-mail: dx2017on@163.com*
*Corresponding author: Xin Du*
*DOI: https://doi.org/10.35633/inmateh-78-12*

***Keywords:*** *Sweet Sorghum Seed; Parameter calibration; RSM; Contact parameters*

## ABSTRACT
*To address the issue of missing discrete element simulation parameters for sweet sorghum seeds, this study systematically calibrated their contact parameters using a method combining physical experiments and numerical simulations. First, a discrete element model of sweet sorghum seeds was constructed via 3D scanning and the multi-sphere filling method, and their basic physical parameters were measured (mean triaxial dimensions: 4.51 mm × 3.20 mm × 2.40 mm, density: 1.156 g/cm³, moisture content: 9.8%). The static friction coefficient (0.303), rolling friction coefficient (0.038), and coefficient of restitution (0.534) between the seeds and polylactic acid (PLA) material were calibrated using inclined plane sliding/rolling tests and free-fall collision tests. Based on the physical test results of the dynamic angle of repose (measured value: 34.61°), the inter-seed static friction coefficient and rolling friction coefficient were screened out as significantly influential parameters via a single factor test. A quadratic regression model was then used to establish a mapping relationship between parameters and the angle of repose, optimizing to obtain the optimal parameter combination (static friction coefficient: 0.124, rolling friction coefficient: 0.020). Simulation verification showed that under this parameter combination, the simulated dynamic angle of repose was 34.59°, with a relative error of only 0.03% compared to the actual value. The parameter calibration method established in this study features high precision and good repeatability, providing reliable parameter support for the discrete element simulation of sweet sorghum sowing equipment, and holding significant engineering application value for optimizing seed metering device design and reducing seed damage rates.*

## 摘要
*针对甜高粱种子离散元仿真参数缺失的问题，本研究通过物理试验与数值模拟相结合的方法，系统标定了其接触参数。首先通过三维扫描和多球填充法构建甜高粱种子离散元模型，并测定其基本物理参数（三轴尺寸均值 4.51 mm×3.20 mm×2.40 mm，密度 1.156 g/cm³，含水率 9.8%）。采用斜面滑动/滚动试验和自由落体碰撞试验，标定种子与聚乳酸（PLA）材料间的静摩擦系数（0.303）、滚动摩擦系数（0.038）和碰撞恢复系数（0.534）。基于动态休止角（实测值 34.61°）的物理试验结果，单因素试验筛选出种子间静摩擦系数、滚动摩擦系数为显著影响参数。通过二次回归模型建立参数与休止角的映射关系，优化得到最优参数组合（静摩擦系数 0.124，滚动摩擦系数 0.020）。仿真验证表明，该参数组合下动态休止角为 34.59°，与实际值相对误差仅 0.03%。本研究建立的参数标定方法精度高、可重复性好，为甜高粱播种机具的离散元仿真提供了可靠参数支持，对优化排种器设计、降低种子破损率具有重要工程应用价值。*

## INTRODUCTION
The discrete element method (DEM) is widely applied to simulate granular materials and predict bulk behaviors such as flowability, piling, and impact response. However, the accuracy of DEM simulations strongly relies on precise contact parameters, including the coefficient of restitution (CR), coefficient of static friction (CSF), and coefficient of rolling friction (CRF). For biological particles like seeds, clarifying collision behavior and obtaining credible restitution and friction-related parameters are essential for reliable modeling (*He et al., 2025*). Despite extensive DEM applications in agriculture, a significant gap remains in the contact parameters for sweet sorghum seeds.

*Xin Du*, Ph.D. Lec.; Jin Yang, Prof. Ph.D.; Zhen Wang, Ph.D. Stud.; Qixin Sun, Prof. Ph.D..*

Numerous studies have demonstrated the importance of parameter calibration for agricultural materials with diverse shapes and mechanical responses. For instance, *Shi et al. (2023)* calibrated bonding parameters and analyzed crushing in brown rice kernels, while *Chen et al.* (*2025*) showed that moisture content significantly affects calibrated parameters in long-grain rice. Beyond rice, calibration frameworks have been developed for irregular particles like tiger nuts (*Shi et al., 2025*), goji berries *(Yu et al., 2022*), hazelnuts (*Wang et al., 2025*), and corydalis tubers (*Liu et al., 2025*), as well as potato minitubers used as seed material (*Chen et al., 2024*). Similar approaches apply to seeds relevant to sowing processes, such as millet seeds (*He et al., 2025*), sorghum seeds (*Mi et al., 2022*), and mixed vetch–oat seeds in pneumatic drilling systems (*Fu et al., 2025)*. These studies confirm that robust parameter calibration is a prerequisite for reliable DEM-based design. Macroscopic calibration targets, like the static or dynamic angle of repose, are commonly used to link micro-contact parameters to observable bulk behavior. For example, repose-angle-based identification has been applied to fresh tea leaves (*Li et al., 2024*), quinoa seed-soil interactions *(Dong et al., 2025*), and complex plant materials requiring additional contact assumptions (*Zhang et al., 2025, Huang et al., 2025*). For flexible materials, model development includes barley seedling stems, wheat straw, and rice straw (*Liu et al., 2025*). At the field scale, calibrated straw-soil models emphasize environmental realism (*Yao et al., 2025*). To improve efficiency, modern workflows combine designed experiments (e.g., Plackett-Burman screening) (*He et al., 2025*) and data-driven methods like BP-neural-network calibration (*Ma et al., 2023*) or GA-BP prediction (*Du and Liu, 2023*). Hybrid optimization-learning approaches (*Du et al., 2021, Du et al., 2022*) and shape simplification (*Wang et al., 2025*) further enhance calibration. However, despite these advances, DEM contact parameters for sweet sorghum seeds are insufficiently established, highlighting a research void in the literature.

To bridge this gap, this study develops a systematic calibration route integrating physical experiments and numerical simulations. The approach consists of three main steps: First, a discrete element model of sweet sorghum seeds is constructed via 3D scanning and multi-sphere filling, with basic physical parameters (e.g., dimensions, density, moisture content) measured experimentally. Second, direct experiments, including inclined plane sliding/rolling tests and free-fall collisions, are used to calibrate seed-material interaction parameters (e.g., with polylactic acid). Third, inter-seed parameters are optimized through bulk-response-driven methods, using the dynamic angle of repose as a calibration benchmark. Single-factor tests and full factorial experiments identify significant parameters, while a quadratic regression model establishes a mapping between parameters and the repose angle. This method ensures high precision and repeatability, providing reliable parameters for simulating sweet sorghum seed behavior in equipment like planters. By building on prior calibration frameworks (*Zhang et al., 2023*), this work offers a tailored solution for sweet sorghum(*Ding et al., 2023*), with potential applications in reducing seed damage and optimizing agricultural machinery.

## MATERIALS AND METHODS

### *DEM modeling of sweet sorghum seed granules*

This research utilized sweet sorghum seeds obtained from Shandong Nongyang Biological Technology Co., Ltd. in China (Fig.1). A random set of 500 seed samples was taken, and their length, width, and thickness were measured along three perpendicular axes using digital calipers with a precision of 0.01 mm. The mean values for length, width, and thickness were determined to be 4.51 mm, 3.20 mm, and 2.40 mm, respectively. Using the provided formula (Equation 1), the equivalent diameter and sphericity of the seeds were computed, yielding results of 3.269 mm and 0.72. From the pre-measured pool, one seed whose dimensions aligned with the calculated averages was chosen. The 3D surface geometry of this selected seed was captured via a 3D scanner and then imported to the EDEM simulation environment. In EDEM, the seed's shape was approximated through an assembly of 21 spheres of different diameters, as illustrated in Figure 1.

$$\begin{cases} D=\sqrt[3]{LWT} \\ S_p = \dfrac{D}{L} \end{cases} \quad (1)$$

where:

$D$ is the equivalent diameter of fertilizer granules, [mm]; $L$ is the length of fertilizer granules, [mm]; $W$ is the width of fertilizer granules, [mm]; $T$ is the thickness of fertilizer granules, [mm]; $S_p$ is the sphericity.

**Fig. 1 - Sweet Sorghum and seed discrete element model**

Three hundred sorghum seeds were randomly chosen for analysis. Their mass and volume were determined via the water displacement method, employing an electronic scale with a precision of 0.001 g and a graduated cylinder accurate to 0.01 mL. Based on these measurements and applying equation (2), the true density of the seeds was derived as 1.156 g/cm³. Separately, the water content of the seeds was found to be 9.8%, as measured by a rapid moisture analyzer with a precision of 0.001 g.

$$\rho_{real} = \frac{m_0}{V_1 - V_0} \tag{2}$$

where: $\rho_{real}$ is the true density of fertilizer particles, [g/cm³]; $m_0$ is the mass of fertilizer particles, [g]; $V_1$ is the total volume of fertilizer particles and water in the measuring cylinder, [cm³]; $V_0$ is the volume of water in the measuring cylinder, [cm³].

The moisture content of sorghum seeds was measured as 12.4% using a rapid moisture analyzer. The coefficient of restitution (CR) between sorghum seeds and polylactic acid (PLA) was determined as 0.534 via a drop test. For the static friction coefficient, three seeds were fixed together with glue and placed on a PLA plate; the plate was gradually inclined until the seeds began to slide, yielding a static friction coefficient of 0.303 between the seeds and PLA. Additionally, multiple seeds were bonded into a sphere with a diameter of 50 mm, which was placed on an inclined plate at 7.2° (as shown in Fig. 2). The rolling distance of the sphere was statistically recorded as 632.8 mm.

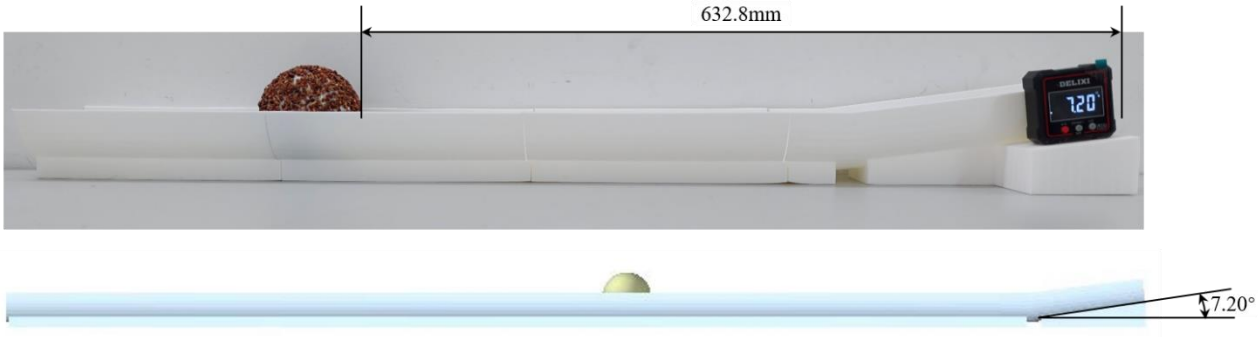


**Fig. 2 – Measurement of CRF between sweet sorghum seeds and PLA**

In the EDEM software, the coefficient of restitution between sorghum seeds and PLA was set to 0.534, and the static friction coefficient was set to 0.303. The inter-particle contact parameters of sorghum seeds were kept at default values, while the rolling friction coefficient range between sorghum seeds and PLA was defined as 0.03–0.04. Based on this, 6 sets of simulation tests were conducted with a friction coefficient gradient of 0.002 (i.e., incrementing by 0.002 per group). The relationship curve between the rolling friction coefficient and horizontal rolling distance in the simulation tests is shown in Fig. 3. By performing quadratic polynomial fitting on the data, the curve equation obtained is:

$$L = 5.844 \times 10^5 x^2 - 6.08 \times 10^4 x + 2097 \tag{3}$$

where:

$L$ represents the measured horizontal rolling distance obtained from the EDEM software, [mm]; $x$ denotes the rolling friction coefficient between sorghum seeds and PLA set in the EDEM software.

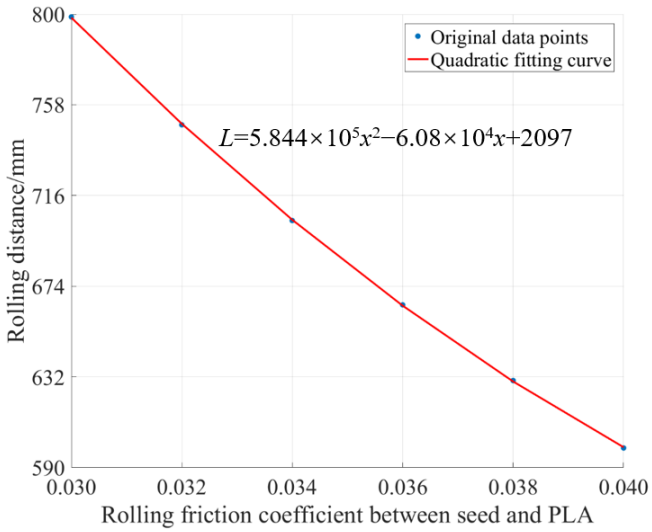


**Fig. 3 – Variation curve of CRF with rolling distance between sweet sorghum seeds and PLA**

The equation demonstrates a high degree of fitting reliability, as indicated by a coefficient of determination ($R^2$) of 0.998. By inputting the experimentally measured horizontal rolling distance of 632.8 mm into Equation (3), the rolling friction coefficient was calculated to be 0.038. Values for the Poisson's ratio (0.25) and the shear modulus ($8.1\times10^8$ Pa) of the sorghum seeds were adopted from previously published research (*Mi et al., 2022*).

***The dynamic angle of repose (DAR) test***

The inter-particle contact coefficient was calibrated using the DAR test, and the actual DAR of the sorghum seeds was measured first. A self-made dynamic angle of repose (DAR) measurement device (as shown in Fig. 4) was employed, equipped with a rotating drum of 90 mm in diameter, 40 mm in width, and a rotation speed of 25 r/min. The main controller was a Raspberry Pi 4B. An image processing workflow was developed based on OpenCV, integrating morphological filtering and an L12-norm linear fitting algorithm. After the seeds flowed stably for 10 seconds, the upper edge features of the irregularly stacked seeds were dynamically extracted in real time, achieving high-precision calculation of the repose angle. The measured dynamic angle of repose was 34.61°.

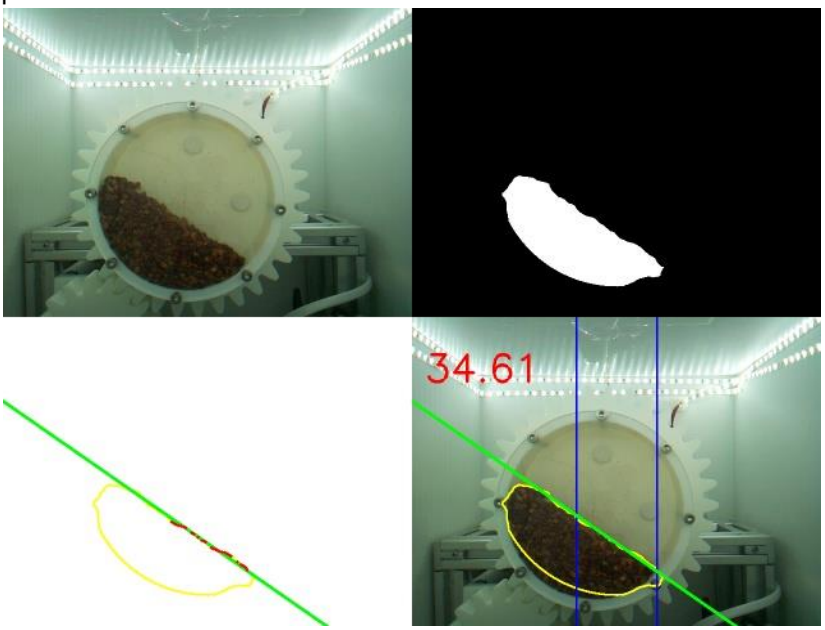


**Fig. 4 - Measurement of DAR in real-world scenarios**

The dynamic angle of repose (DAR) for sorghum seeds was simulated numerically using EDEM 2023 software, as depicted in Figure 5. A rotating drum apparatus (shown in Fig. 5) was employed in the simulation to capture the inter-seed interactions accurately. The drum was loaded with 200 g of seeds for the test. The simulation was conducted over a total duration of 12 seconds, utilizing a fixed time step of $5\times10^{-6}$ seconds. Upon completion of the simulation, post-processing was performed by executing a custom DAR analysis program. This was achieved by utilizing Python 3.6 to call functions from the EDEMpy library. Within this program, four sampling surfaces were defined across the surface of the seed pile. The positional data of seeds contacting these surfaces was extracted, subjected to linear fitting, and used to compute and output both the average DAR value and its standard deviation.

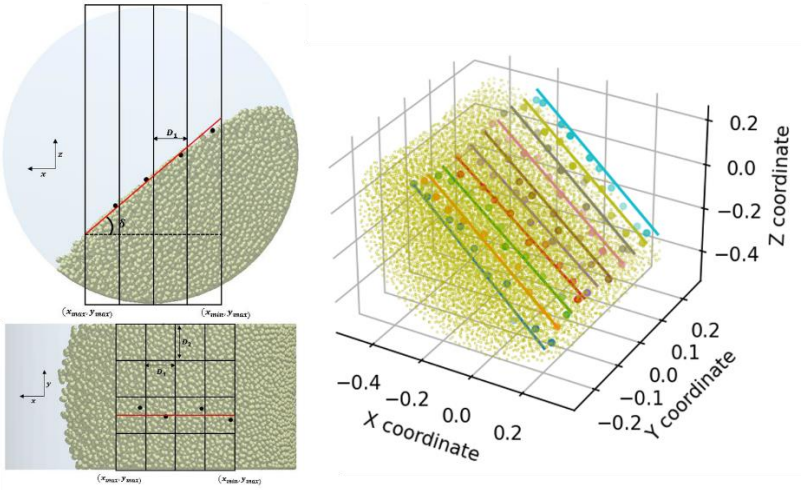


**Fig. 5 – Measurement of DAR in simulation**

## RESULTS

### *Coefficient of restitution (CR)*

For the simulation involving sorghum seeds, the static friction coefficient (CSF) was specified as 0.13 and the rolling friction coefficient (CRF) as 0.01. The coefficient of restitution (CR) was examined over a horizontal interval spanning from 0.2 to 0.6, with a step size of 0.1 between levels.

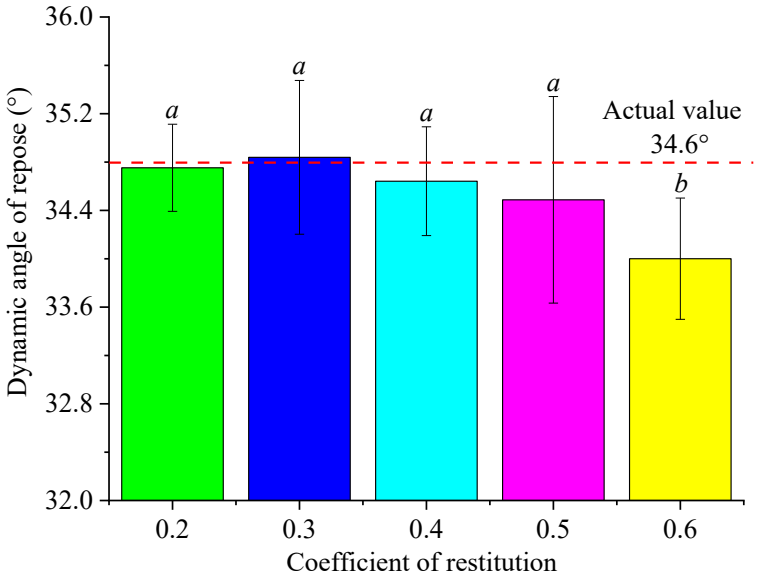


**Fig. 6 –Effect of CR between seeds on DAR**

Figure 6 illustrates how the dynamic angle of repose (DAR) of the sorghum seeds changes across the tested gradient of coefficients of restitution (CR) between seeds. The ANOVA yielded a significance level of $P < 0.0001$, demonstrating that the inter-seed CR has a statistically significant effect on the measured DAR. As shown, the DAR exhibits a decreasing trend as the CR increases. Post-hoc analysis revealed that while the differences in DAR were not significant among CR levels of 0.2, 0.3, 0.4, and 0.5, a significant difference was detected between the groups at CR=0.5 and CR=0.6. Based on the experimental data, the actual CR value corresponding to the physical DAR measurement is estimated to fall within the range of 0.2 to 0.4.

***Coefficient of static friction (CSF)***

For this set of simulations, the coefficient of restitution (CR) and the coefficient of rolling friction (CRF) between sorghum seeds were fixed at 0.2 and 0.01, respectively. The coefficient of static friction (CSF) was varied across a horizontal range from 0.11 to 0.15, with increments of 0.01.

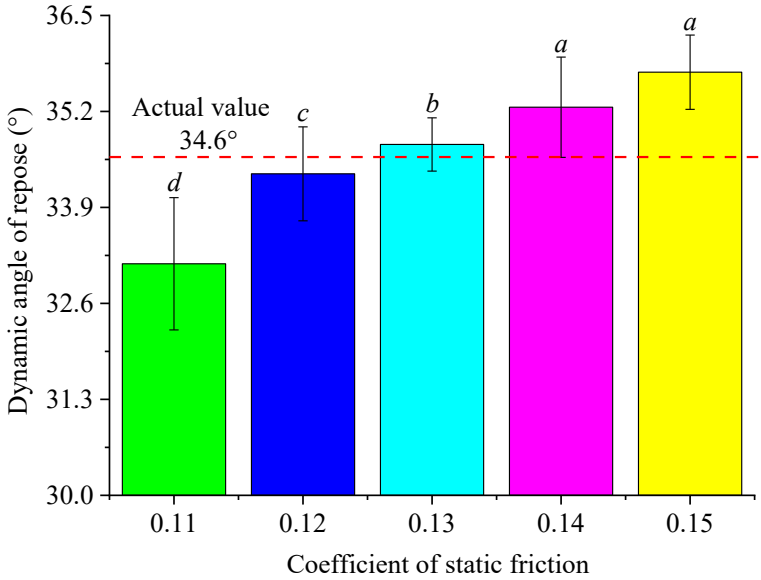


**Fig. 7 – Effect of CSF between seeds on DAR**

The relationship between the dynamic angle of repose (DAR) and each level of the inter-seed CSF is presented in Figure 7. The ANOVA results showed that the effect of the inter-seed CSF on the DAR was highly significant, with the analysis returning a P-value of less than 0.0001. As observed, the DAR exhibited a positive correlation with the inter-seed CSF; it increased as the CSF value increased. Post-hoc comparisons indicated that the differences in DAR were significant across CSF levels ranging from 0.11 to 0.14. However, no significant difference was found between the DAR values at CSF levels of 0.14 and 0.15. By comparing the simulation results with the physical measurement, the CSF value corresponding to the actual DAR was estimated to lie within the interval of 0.12 to 0.14.

***Coefficient of rolling friction (CRF)***

In this series of simulations, the coefficient of restitution (CR) and the coefficient of static friction (CSF) between sorghum seeds were held constant at 0.2 and 0.13, respectively. The coefficient of rolling friction (CRF) was assigned values across an interval from 0.004 to 0.020, with a uniform increment of 0.004 between levels.

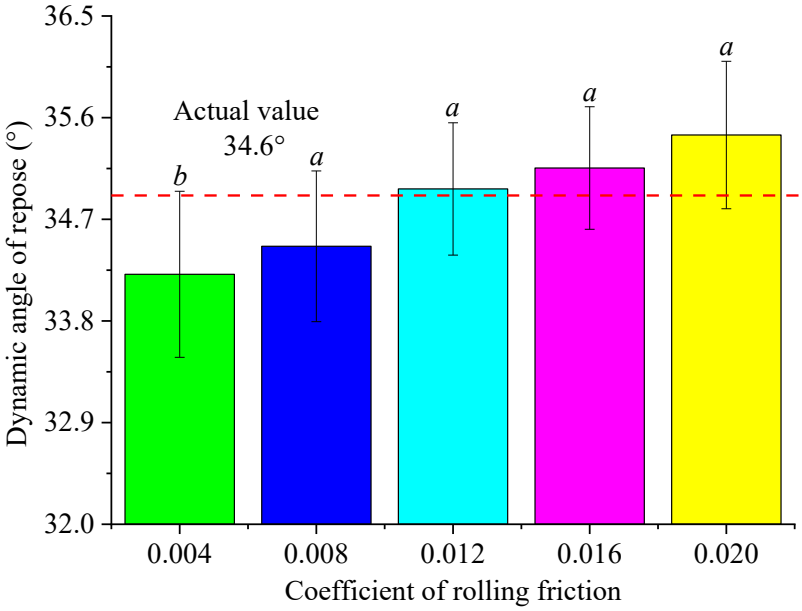


**Fig. 8 – Effect of CRF between seeds on DAR**

The response of the dynamic angle of repose (DAR) to these varying CRF levels is displayed in Figure 8. The analysis revealed a highly significant effect of the inter-seed CRF on the DAR ($P < 0.0001$). Visually, the DAR shows an upward trend as the CRF increases. Post-hoc testing demonstrated that the differences in DAR were statistically significant for CRF values between 0.004 and 0.008. In contrast, no significant differences were observed among DAR groups when the CRF was within the range of 0.008 to 0.020. By aligning the simulation outcomes with the experimentally measured DAR, the corresponding inter-seed rolling friction coefficient was calibrated to a value between 0.008 and 0.016.

***Full factorial experiment***

Based on the above analysis, the collision recovery coefficient (CR) between sorghum seeds has no significant effect on the dynamic angle of repose (DAR) and shows no clear pattern. Thus, the CR between sorghum seeds was fixed at 0.2. To investigate the influence pattern of the interaction between inter-seed contact parameters (CSF, CRF) on the DAR, five levels were set for both CSF and CRF, and a two-factor full factorial experiment with five levels per factor was conducted. The experimental results are shown in Table 1.

**Table 1**

**Test plan and results**

| Number | CSF $x_1$ | CRF $x_2$ | DAR y (°) | StDev (°) |
|---|---|---|---|---|
| 1 | 0.11 | 0.004 | 32.55 | 0.67 |
| 2 | 0.11 | 0.008 | 33.37 | 0.59 |
| 3 | 0.11 | 0.012 | 33.54 | 0.70 |
| 4 | 0.11 | 0.016 | 33.46 | 0.67 |
| 5 | 0.11 | 0.020 | 33.75 | 0.54 |
| 6 | 0.12 | 0.004 | 32.99 | 0.75 |
| 7 | 0.12 | 0.008 | 33.86 | 0.45 |
| 8 | 0.12 | 0.012 | 33.88 | 0.82 |
| 9 | 0.12 | 0.016 | 34.45 | 0.86 |
| 10 | 0.12 | 0.020 | 33.99 | 0.71 |
| 11 | 0.13 | 0.004 | 34.13 | 0.61 |
| 12 | 0.13 | 0.008 | 34.27 | 0.62 |
| 13 | 0.13 | 0.012 | 34.34 | 0.46 |
| 14 | 0.13 | 0.016 | 34.84 | 0.66 |
| 15 | 0.13 | 0.020 | 34.95 | 0.88 |
| 16 | 0.14 | 0.004 | 34.76 | 0.59 |
| 17 | 0.14 | 0.008 | 35.09 | 0.67 |
| 18 | 0.14 | 0.012 | 35.43 | 0.71 |
| 19 | 0.14 | 0.016 | 35.32 | 0.55 |
| 20 | 0.14 | 0.020 | 35.77 | 0.56 |
| 21 | 0.15 | 0.004 | 35.23 | 0.49 |
| 22 | 0.15 | 0.008 | 35.16 | 0.72 |
| 23 | 0.15 | 0.012 | 35.86 | 0.43 |
| 24 | 0.15 | 0.016 | 36.27 | 0.84 |
| 25 | 0.15 | 0.020 | 36.52 | 0.55 |

With the dynamic angle of repose (DAR) as the response variable, a second-order polynomial regression was applied to the experimental data. This process established a quadratic model that describes the relationship between the DAR and the contact parameters—specifically, the coefficient of static friction (CSF) and the coefficient of rolling friction (CRF)—thereby elucidating their respective influence patterns on the DAR.

$$y = 27.91 + 27.32x_1 + 62.36x_2 + 514x_1x_2 + 116.9x_1^2 - 2621x_2^2 \quad (4)$$

The goodness-of-fit for the DAR regression model was evaluated, yielding a sum of squared errors (SSE) of 0.04572, a root mean square error (RMSE) of 0.04906, and a coefficient of determination ($R^2$) of 0.9997. These results demonstrate that the regression model is statistically highly significant and provides an excellent fit to the experimental data. Consequently, the derived formula is reliable and can be used to inversely determine the corresponding CSF and CRF values for any given target DAR.

The interactive effect of DAR on CSF and CRF is shown in Fig. 9.

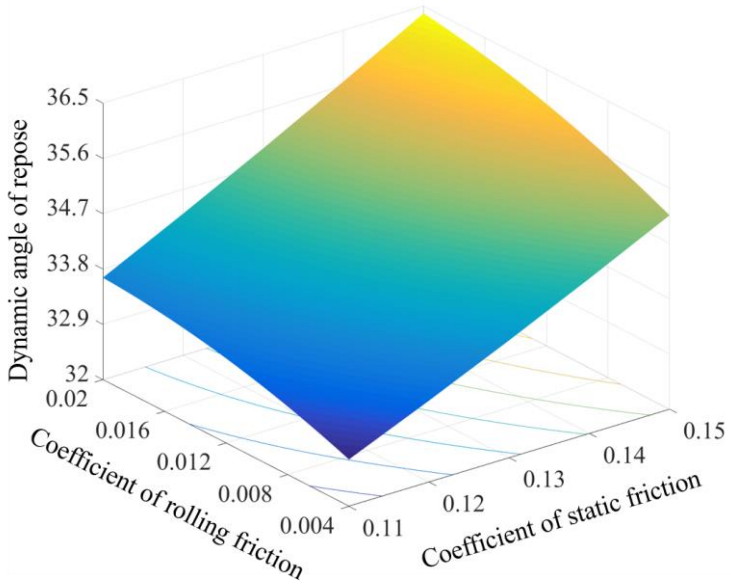


**Fig. 9 – Effect of the interaction between CSF and CRF on DAR**

Figure 10 illustrates a curve (depicted by the black line) that is derived from Equation (4). This curve represents all possible combinations of the coefficient of static friction (CSF) and the coefficient of rolling friction (CRF) that theoretically result in a dynamic angle of repose (DAR) of 34.6°. As implied by the continuous curve, an infinite number of such CSF-CRF pairs exist. For verification, five points were arbitrarily chosen along this curve, corresponding to CRF values of 0.004, 0.008, 0.012, 0.016, and 0.020. These five distinct parameter sets were subsequently used as inputs for simulations conducted in EDEM software. The outcomes of these simulations are presented in Figure 11.

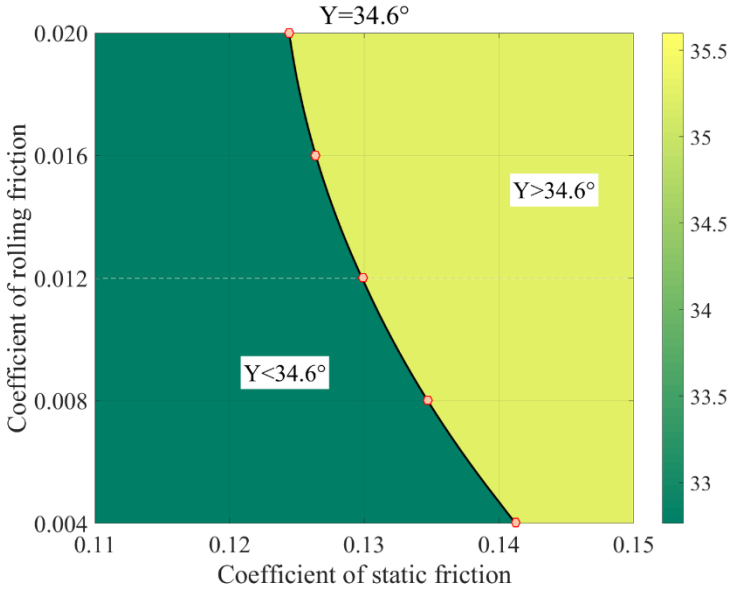


**Fig. 10 – Effect of the values of CSF and CRF on the magnitude of DAR**

As shown in Fig. 11, all errors between the simulated DAR values and the actual value (34.6°) were less than 1%. Notably, when CSF=0.124 and CRF=0.020, the simulated DAR was 34.59°, with a relative error of only 0.03% compared to the actual value (34.6°).

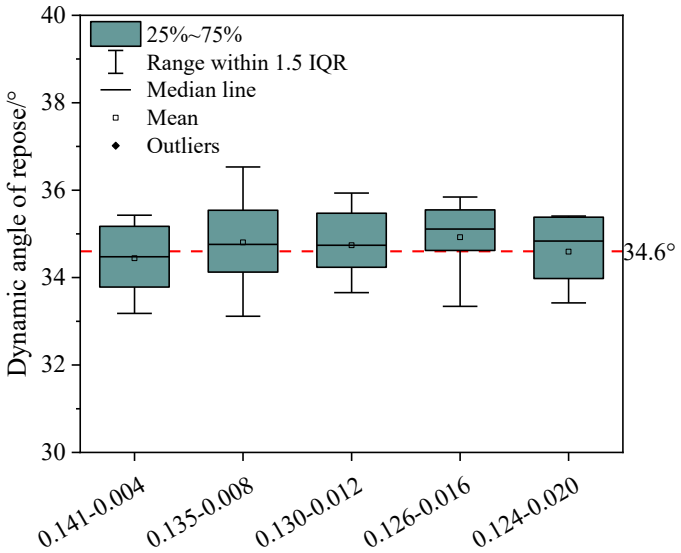


**Fig. 11 – Distribution of simulated DAR under different parameter combinations of CSF and CRF**

The dynamic stacking state of sorghum seeds during rolling at this parameter combination is shown in Fig. 12. It can be observed that the stacking states were nearly identical, indicating that the measured and simulated parameters are reliable and can reflect the actual motion characteristics of sorghum seeds.

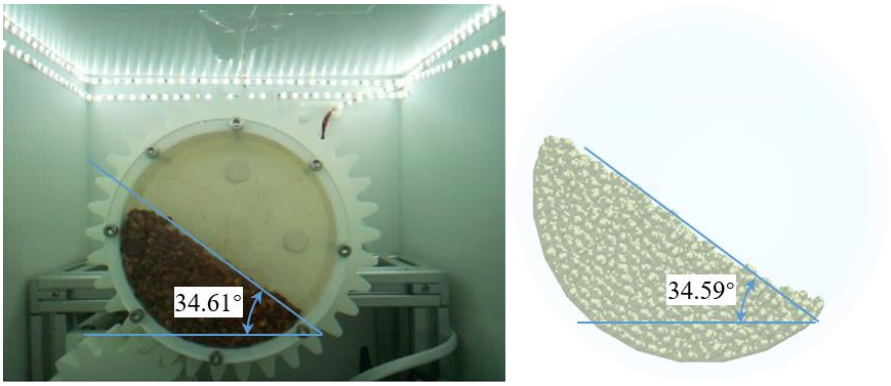


**Fig. 12 – Comparison between experiments and simulated DAR**

## CONCLUSIONS

The research aimed to calibrate DEM contact parameters—specifically, the coefficient of restitution (CR), coefficient of static friction (CSF), and coefficient of rolling friction (CRF)—for sweet sorghum seeds. This was achieved by combining physical experiments (e.g., measuring seed dimensions, density, and moisture content) with EDEM software simulations, using the dynamic angle of repose (DAR) as a calibration benchmark. The actual DAR was measured as 34.61° in real-world tests.

Sweet sorghum seeds had an average triaxial size of 4.51 mm × 3.20 mm × 2.40 mm, equivalent diameter of 3.269 mm, sphericity of 0.72, true density of 1.156 g/cm³, and moisture content of 9.8%. Parameters for seed-PLA interaction were determined: CR = 0.534, CSF = 0.303, and CRF = 0.038 (based on a rolling distance of 632.8 mm).

Single-factor tests showed that DAR decreases with increasing CR but increases with CSF and CRF. ANOVA results ($P < 0.0001$) confirmed significant effects. A full factorial experiment with CSF and CRF revealed their interaction, leading to a quadratic regression model (Equation 3) with high accuracy ($R^2 = 0.9997$, RMSE = 0.04906). For a target DAR of 34.6°, multiple CSF-CRF combinations form a continuous curve, demonstrating parameter multiplicity. Simulations using five points on this curve (e.g., CSF=0.124, CRF=0.020) yielded DAR errors below 1%, with a minimum error of 0.03%.

The calibrated parameters were validated through comparisons between real and simulated seed stacking states, showing nearly identical flow characteristics. This confirms the reliability of the method for simulating seed motion in agricultural equipment design, such as planters and conveyors.

**ACKNOWLEDGEMENT**

This study was supported by the Youth Fund of Natural Science Foundation of Jiangsu Province (BK20241058), Lianyungang City Key Research and Development Project (Social Development) (SF2439) and Lianyungang City Transformation of Scientific and Technological Achievements Unveiling the List and Appointing the Leader Project (CA202303).

## REFERENCES

[1] Chen, K., Yin, X., Ma, W., Jin, C., Liao, Y. (2024). Contact Parameter Calibration for Discrete Element Potato Minituber Seed Simulation. *Agriculture*, Vol. 14, pp. 2298. DOI: https://doi.org/10.3390/agriculture14122298

[2] Chen, Z., Che, G., Wan, L., Wang, H., Zhang, K. (2025). Calibration and Experimental Validation of Discrete Element Parameters for Long-Grain Rice with Different Moisture Contents Based on Repose Angle. *Agriculture*, Vol. 15, pp. 1058. DOI: https://doi.org/10.3390/agriculture15101058

[3] Ding, X., Wang, B., He, Z., Shi, Y., Li, K., Cui, Y., Yang, Q. (2023). Fast and Precise DEM Parameter Calibration for Cucurbita ficifolia Seeds. *Biosystems Engineering*, Vol. 236, pp. 258-276. DOI: https://doi.org/10.1016/j.biosystemseng.2023.11.004

[4] Dong, W., Zhao, X., Liu, F., Bai, H., Xuan, D., Zhang, A., Ren, Y. (2025). Establishment and Parameter Calibration of Quinoa Seed-Soil Contact Model Based on Discrete Element Method. *INMATEH - Agricultural Engineering*, Vol. 76, no. 2, pp. 872-885, DOI: https://doi.org/10.35633/inmateh-76-75

[5] Du, X., Liu, C. Prediction of DEM Parameters of Coated Fertilizer Particles Based on GA-BP Neural Network. (2023). *Engenharia Agrícola*, Vol. 43 (special issue): e20210099. DOI: http://dx.doi.org/10.1590/1809-4430-Eng.Agric.v43nepe20210099/2023

[6] Du, X., Liu, C., Jiang, M., Yuan, H., Dai, L., Li, F., Gao, Z. (2021). Calibration of Bonding Model Parameters for Coated Fertilizers Based on PSO-BP Neural Network. *INMATEH - Agricultural Engineering*, Vol. 65, no. 3, pp. 255-264. DOI: https://doi.org/10.35633/inmateh-65-27

[7] Du, X., Liu, C., Jiang, M., Yuan, H., Dai, L., Li, F., Gao, Z. (2022). Research on DEM Calibration of Contact Parameters of Coated Fertilizer. *INMATEH-Agricultural Engineering*, Vol. 66, no.1, pp. 101-110. DOI: https://doi.org/10.35633/inmateh-66-10

[8] Fu, Y., Wang, D., Wang, X., Wang, L., Hu, J., Chi, X., Ji, M. (2025). Parameter Calibration and Experimentation of the Discrete Element Model for Mixed Seeds of Vetch (Vicia villosa) and Oat (Avena sativa) in a Pneumatic Seed Drilling System. *Applied Sciences*, Vol. 15, pp. 13048, Alar/China. DOI: https://doi.org/10.3390/app152413048

[9] He, Y., Ji, X., Dun, G., Liu, X., Mu, A., Ma, C. (2025). Discrete Element Simulation Calibration of Contact Parameters for Millet Seeds. *INMATEH-Agricultural Engineering*, Vol. 76, no.2, pp. 686-696. DOI: https://doi.org/10.35633/inmateh-76-58

[10] He, Z., Wang, M., Zhao, Z., Xie, Y., Liu, M. (2025). A Study on the Influencing Factors of Corn Kernel Collision Restitution Coefficient Based on the Oblique Impact Collision Theory. *INMATEH - Agricultural Engineering*, Vol. 76, no.2, pp. 840-850. DOI: https://doi.org/10.35633/inmateh-76-72

[11] Huang, H., Zhang, Y., Hou, G., Su, B., Yin, H., Fu, Z., Zhuang, Y., Lv, Z., Tian, H., Li, L. (2025). Establishment of Hollow Flexible Model with Two Types of Bonds and Calibration of the Contact Parameters for Wheat Straw. *Agriculture*, Vol. 15, pp. 1686. DOI: https://doi.org/10.3390/agriculture15151686

[12] Li, D., Wang, R., Zhu, Y., Chen, J., Zhang, G., Wu, C. (2024). Calibration of Simulation Parameters for Fresh Tea Leaves Based on the Discrete Element Method. *Agriculture*, Vol. 14, pp. 148. DOI: https://doi.org/10.3390/agriculture14010148

[13] Liu, G., Wang, K., Chen, X., Gong, J., Deng, Z., Li, B. (2025). Research on Contact Parameter Calibration and Experiment of Discrete Element Simulation Model for Rice Straw. *INMATEH - Agricultural Engineering*, Vol. 77, no. 3, pp. 215-226. DOI: https://doi.org/10.35633/inmateh-77-17

[14] Liu, X., Wang, C., Shao, Y., Zhang, W. (2025). Discrete Element Modeling and Parameter Calibration for Corydalis Tuber. *INMATEH-Agricultural Engineering*, Vol. 76, no. 2, pp. 26-37. DOI: https://doi.org/10.35633/inmateh-76-02

[15] Liu, Z., Yan, J., Liu, F., Wang, L. (2025). Calibration and Testing of Discrete Element Simulation Parameters for the Presoaked Cyperus esculentus L. Rubber Interface Using EDEM. *Agronomy*, Vol. 15, pp. 2440. DOI: https://doi.org/10.3390/agronomy15102440

[16] Ma, X., Guo, M., Tong, X., Hou, Z., Liu, H., Ren, H. (2023). Calibration of Small-Grain Seed Parameters

Based on a BP Neural Network: A Case Study with Red Clover Seeds. *Agronomy*, Vol. 13, pp. 2670. DOI: https://doi.org/10.3390/agronomy13112670

[17] Mi, G., Liu, Y., Wang, T., Dong, J., Zhang, S., Li, Q., Chen, K., Huang, Y. (2022). Measurement of Physical Properties of Sorghum Seeds and Calibration of Discrete Element Modeling Parameters. *Agriculture*, Vol. 12, p. 681. DOI: https://doi.org/10.3390/agriculture12050681

[18] Shi, Y., Zhang, X., Yan, J., Ma, X., Li, H., Han, C. (2025). Calibration and Optimization of Discrete Element Parameters for Tiger Nuts. *INMATEH-Agricultural Engineering*, Vol. 76, no. 2, pp. 978-993. DOI: https://doi.org/10.35633/inmateh-76-84

[19] Shi, Z., Liu, X., Zhang, Y., Zhou, J., Li, H., Duan, F. (2023). Bond Parameter Calibration and Crushing Process Analysis of Brown Rice Kernels. *Processes*, Vol. 11, pp. 2992. DOI: https://doi.org/10.3390/pr11102992

[20] Wang, C., Kui, H., Wu, X., Shao, Y., Fu, M. (2025). DEM-Based Modeling and Contact Parameter Calibration of Hazelnuts. *INMATEH-Agricultural Engineering*, Vol. 76, no. 2, pp. 829-839. DOI: https://doi.org/10.35633/inmateh-76-71

[21] Wang, J., Geng, B., Yang, Z., Yang, J., Zhang, K., Meng, Y. (2025). Discrete Meta-Modeling and Parameter Calibration of Harvested Alfalfa Stalks. *Agronomy*, Vol. 15, pp. 2390. DOI: https://doi.org/10.3390/agronomy15102390

[22] Wang, X., Zhou, H., Geng, D., Zha, Z., Li, Z. (2025). Discrete Element Parameter Calibration and Optimization of Laminaria japonica Based on GP-PSO-XGBOOST Model. *INMATEH - Agricultural Engineering*, Vol. 76, no. 2, pp. 638-651. DOI: https://doi.org/10.35633/inmateh-76-54

[23] Wang, Z., Hou, Z., Bao, L., Liu, Y., Li, B., Guo, F. (2025). Construction of Ellipsoidal Particle Discrete Element Model and Calibration of Simulation Parameters. *INMATEH - Agricultural Engineering*, Vol. 77, no. 3, pp. 1362-1372. DOI: https://doi.org/10.35633/inmateh-77-108

[24] Yao, W., Miao, H., Chen, M., Diao, P., Xu, G. (2025). Parameter Calibration and Validation of a Straw-Soil Discrete Element Model in Huang-Huai-Hai Wheat Stubble Fields. *INMATEH - Agricultural Engineering*, Vol. 77, no. 3, pp. 350-361. DOI: https://doi.org/10.35633/inmateh-77-28

[25] Yu, Y., Ren, S., Li, J., Chang, J., Yu, S., Sun, C., Chen, T. (2022). Calibration and Testing of Discrete Element Modeling Parameters for Fresh Goji Berries. *Applied Sciences*, Vol. 12, pp. 11629. DOI: https://doi.org/10.3390/app122211629

[26] Zhang, J., Chang, Z., Niu, F., Chen, Y., Wu, J., Zhang, H. (2023). Simulation and Validation of Discrete Element Parameter Calibration for Fine-Grained Iron Tailings. *Minerals*, Vol. 13, pp. 58. DOI: https://doi.org/10.3390/min13010058

[27] Zhang, X., Tao, G., Xu, Y., Yu, C. (2025). Construction and Parameter Calibration of a Discrete Element Model of Barley Seedling Stems. *INMATEH - Agricultural Engineering*, Vol. 77, no. 3, pp. 30-43. DOI: https://doi.org/10.35633/inmateh-77-03